Available online at www.sciencedirect.com
SCIENCE DIRECT®
Journal of Solid State Chemistry 177 (2004) 4351–4358
JOURNAL OF SOLID STATE CHEMISTRY
http://elsevier.com/locate/jssc

Synthesis, structure, and properties of chromium(III) sulfates

Tom David Atkinson, Helmer Fjellvåg, and Arne Kjekshus*

Department of Chemistry, University of Oslo, P.O. Box 1033, Blindern, N-0315 Oslo, Norway

Received 21 January 2004; accepted 25 March 2004

Abstract

Reactions between CrO_3 and 50–95 wt% H_2SO_4 are studied at temperatures up to the boiling point of the acid. Depending on the H_2SO_4 concentration and synthesis temperature, $Cr_2(SO_4)_3$, $CrH(SO_4)_2$, $(H_3O)[Cr(SO_4)_2]$, $Cr_2(SO_4)_3 \cdot H_2SO_4 \cdot 4H_2O$ (gross formula), and $(H_5O_2)[Cr(H_2O)_2(SO_4)_2]$, are obtained as identified reaction products in addition to the incompletely characterized chromic–sulfuric acid. The Cr^{III}-based sulfates are characterized by X-ray powder diffraction, thermogravimetric, and magnetic susceptibility measurements. The nuclear and magnetic structures of $Cr_2(SO_4)_3$ at 10 K are determined, the structure type of $(H_3O)[Cr(SO_4)_2]$ is established, and the crystal structure of $(H_5O_2)[Cr(H_2O)_2(SO_4)_2]$ is firmly stipulated. Magnetic susceptibility data suggest that the samples of $CrH(SO_4)_2$ are in a micro-crystalline rather than in an amorphous state. All Cr^{III}-based sulfates synthesized in this study appear to undergo paramagnetic-to-antiferromagnetic transitions at around 10 K.

Keywords: Synthesis in concentrated sulfuric acid; Cr^{III}-based sulfates; Magnetic properties of Cr^{III}-based sulfates; Magnetic structure of $Cr_2(SO_4)_3$

1. Introduction

Chromium sulfates have attracted the attention of the chemists for a couple of centuries. For example, the popularity of chromic–sulfuric acid as a cleaning solution for analytic–chemical glassware is reflected in frequent studies of the CrO_3–SO_3–H_2O system. Von Bolley [1] observed already in 1845 that hot concentrated sulfuric acid can dissolve considerable amounts of CrO_3, giving an oily, dark-brown solution which after about a day obtains granular appearance and turns red on exposure to moist air. Von Bolley suggested that the original product had the composition $CrO_3 \cdot SO_3 \cdot H_2O$ ($= H_2CrSO_7$).

Rakowsky and Tarassenkow [2] considered the earlier knowledge [1,3–8] on the CrO_3–SO_3–H_2O system as incomplete, and these authors therefore took on a systematic study of the phase diagram between 0°C and 100°C. The findings of Rakowsky and Tarassenkow are still today regarded as a reliable source for information on the CrO_3–SO_3–H_2O system. However, these authors seem to have arrived at an incorrect formula for the intermediate phase of the system ($CrO_3 \cdot SO_3$ instead of $CrO_3 \cdot SO_3 \cdot H_2O$). In fact, on critical comparison of all data in Refs. [1–8] it is possible to explain many of the mutual divergences as smaller or larger deviations in the preparational procedures.

Systematic studies on the outcome when CrO_3–SO_3–H_2O mixtures are heated above 100°C are not available, and the purpose of this communication is to contribute to some rectification of this shortage. The effect which sets in above 100°C is the decomposition of CrO_3 to Cr_2O_3 and O_2. The onset temperature for detectable decomposition is distinctly lower for CrO_3 admixed with concentrated H_2SO_4 (reaction rate dependent on H_2SO_4 concentration, partial pressure of O_2, and additives like Cr^{3+} in addition to temperature) than for the degradation of pure CrO_3 [9–11]. As to whether Cr_2O_3 really appears as a separable intermediate reduction product in concentrated H_2SO_4 is not firmly established [11]. The compositions of the final products of reactions between hot concentrated H_2SO_4 and CrO_3 are also debated over the years [1–14]. The formula $Cr_2(SO_4)_3$ for the product formed at the highest H_2SO_4 concentrations now seems well documented [15–17], but the debate on whether there occur two modifications of this compound is not definitely settled. Below an H_2SO_4 concentration of

*Corresponding author. Fax: +47-2-285-5541.
E-mail address: arne.kjekshus@kjemi.uio.no (A. Kjekshus).

0022-4596/$ - see front matter © 2004 Elsevier Inc. All rights reserved.
doi:10.1016/j.jssc.2004.03.038

some 90 wt% the products appear to be hydrates of chromium(III) sulfate and/or protonated derivatives thereof, and the discussion touches upon just the amount of "crystal water" and to which part of the structural framework the protons are connected. The present contribution also aims at bringing a little more clarity on these points.

2. Experimental

2.1. Synthesis

CrO_3 (Fluka, $\geqslant$99.0%) and conc. H_2SO_4 (Merck, 95–97 wt%; the former value being used throughout this paper) were used as starting chemicals for the syntheses. Concentrated H_2SO_4 in the range 50–95 wt% was made by diluting the as-purchased acid with distilled water. The concentration of these acids was checked using a densitometric flask and confirmed by comparing the measured densities with published values [18]. CrO_3 was added to 20 mL conc. H_2SO_4 (50–95 wt%) in a round-bottomed flask equipped with either a glass stopper for reactions near room temperature (r.t.) or a reflux cooler for reactions at higher temperatures. The molar ratio [Cr]:[H_2SO_4] for the starting mixtures was 1:20 for 70–95 wt% H_2SO_4, but was gradually increased to 1:2 between 70 and 50 wt%. The mixtures were stirred with a magnetic stirrer and treated at different temperatures from r.t. to the boiling point for periods from 15 min to 6 months. For temperatures up to 100°C the heating was supplied from a water bath, a silicon-oil bath was used between 100°C and 210°C and above 210°C the reaction vessel (wrapped with Al foil) was placed directly on the heating plate. The reaction temperature was recorded both with a thermometer brought in through the cooler and another on the outside of the glass flask in level with the reaction mixture. (The latter precaution was taken because the consistency of the reaction mixture, in some cases, precluded direct contact with the inside thermometer.) After the heating and stirring had been turned off the reaction vessel was left untouched (for at least 1 day) until the product was well separated from the saturated H_2SO_4 motherliquid. The liquid phase was then removed by decantation. The product was subsequently transferred to a beaker containing 100 mL glacial acetic acid (Merck) and stirred for 10 min. The product was filtered off and successively washed with 50 mL glacial acetic acid, 50 mL acetone (Prolab), and 50 mL diethyl ether (Den norske Eterfabrikk), and then transferred to a desiccator for drying and storing under ambient conditions.

Single-crystal specimens of $Cr_2(SO_4)_3$ (used for magnetic susceptibility measurements) were prepared by chemical transport reactions. Micro-crystalline (according to powder X-ray diffraction (PXD), see below) $Cr_2(SO_4)_3$ was used as source and HCl (gas at 1 atm and 25°C on filling) as transport agent, contained in 100 mm long, 15 mm bore silica–glass capsules which were subjected to a 700-to-600°C temperature gradient. The transported material after 48 day constituted only a small fraction of the amount expected according to transport-rate data reported by Dahmen and Gruehn [17].

$Cr_2(SO_4)_3 \cdot 14H_2O$ was prepared according to the procedure of Traube [19]: Freshly recrystallized CrO_3 was dissolved in appropriately diluted H_2SO_4 and subjected to an atmosphere of diethyl ether for 1 day. The resulting slow reduction and precipitation reaction leads to well-defined crystals of $Cr_2(SO_4)_3 \cdot 14H_2O$. The reduction reaction may be completed by slow addition of ethanol (to excess).

2.2. Powder X-ray and neutron diffraction refinements

All samples were characterized by PXD (Cu$K\alpha_1$ radiation, Si as internal standard) at 25°C using either a Guinier–Hägg camera or a Siemens D5000 diffractometer in transmission geometry (in many cases both techniques were utilized). The position of the Bragg reflections for the film-technique data was measured by a Nicolet L18 scanner using the SCANPI [20] program system. The diffractometer data were recorded with a Brown PSD. The diffraction patterns were collected over the 2θ range 80–90° and autoindexed with help of the TREOR [21] program. Unit-cell dimensions (calibrated to silicon standard) were obtained by least-squares refinements using the CELLKANT [22] and/or ITO [23] programs.

PXD data for the structure refinement of $Cr_2(SO_4)_3 \cdot H_2SO_4 \cdot 8H_2O$ {viz. $2(H_5O_2)[Cr(H_2O)_2(SO_4)_2]$ see below} were collected at the Swiss–Norwegian Beam Line BM01 at ESRF, Grenoble. Data were recorded in the Debye–Scherrer mode using photons of wavelength 0.80202 Å obtained from an Si(111) channel-cut monochromator (range $2\theta = 4.5$–46.49°, in steps of 0.002°). High-temperature PXD data for $Cr_2(SO_4)_3 \cdot H_2SO_4 \cdot 8H_2O$ were collected with a Guinier–Simon camera between 20°C and 500°C.

High-resolution powder neutron diffraction (PND) data for $Cr_2(SO_4)_3$ were collected at 10 K (obtained with a Displex cooler) with the PUS two-axis diffractometer [$\lambda = 1.555$ Å, focussing Ge(511) monochromator] accommodated at the JEEP II reactor, Kjeller, Norway. The sample was contained in a cylindrical vanadium holder with 3 mm inner diameter. The diffraction pattern was registered by means of two detector banks, each covering 20° in 2θ and each containing a stack of seven position-sensitive detectors [24] (total 2θ range covered: 10–130°, step length: 0.05°).

The Rietveld refinements of the synchrotron PXD data for $Cr_2(SO_4)_3 \cdot H_2SO_4 \cdot 8H_2O$ were performed with

the program DBW3.2S [25]. The GSAS [26] software was used for the Rietveld refinements of the nuclear and magnetic structures of $Cr_2(SO_4)_3$ on the basis of PND data. The nuclear scattering lengths and the magnetic form factor for Cr were taken from the GSAS library. The background was modeled as a cosine Fourier series polynomial (12 terms) and the peak shape was modeled as a pseudo-Voigt function.

2.3. Magnetic susceptibility

Magnetic-susceptibility measurements were performed in the temperature range 3–325 K using a superconducting quantum-interference-device instrument (Magnetic Property Measurement System; Quantum Design) with 10–30 mg samples and a magnetic field of 500 Oe. (Test scans of magnetization versus field strength were made up to 5.5 T at 5 and 100 K.)

2.4. Thermoanalysis

Thermogravimetric (TG) analysis was performed between 20°C and 1000°C with a Perkin Elmer TGA7 system. Silica–glass containers were used as sample holders, the heating rate was 2–10°C min^{-1} and flowing nitrogen was used as atmosphere.

3. Results and discussion

3.1. Syntheses and product characterization

As pointed out in Ref. [27] several parameters, which are involved during syntheses in concentrated H_2SO_4 and characterization of their outcome, may have influenced the products. The present study has focused on the effects on the products by H_2SO_4 concentration, reaction temperature, reaction time, and [Cr]:[H_2SO_4] ratio. These parameters were varied one at the time, and the results are summarized in Fig. 1. Although this illustration is based on some 100 different experiments it should be emphasized that the positioning of the boundaries between the different product phase fields should be regarded as rather approximate.

Up to about 60 wt% H_2SO_4 and some 120°C no sign of any reaction is seen and the remaining solid after very long reaction periods was definitely CrO_3. At lower temperatures this situation is maintained to still higher H_2SO_4 concentrations, but when the H_2SO_4 concentration approaches 90 wt% a noticable reaction is easily detectable even at r.t. by changes in the color of the reaction mixture. For a typical experiment at 100°C and 95 wt% H_2SO_4 the mixture turns from red-brown to brown-red during the first hour, has become light brown after 2 h, dark brown after 3 h, and still darker colored with a greenish stain after 7 days. Treatment for up to

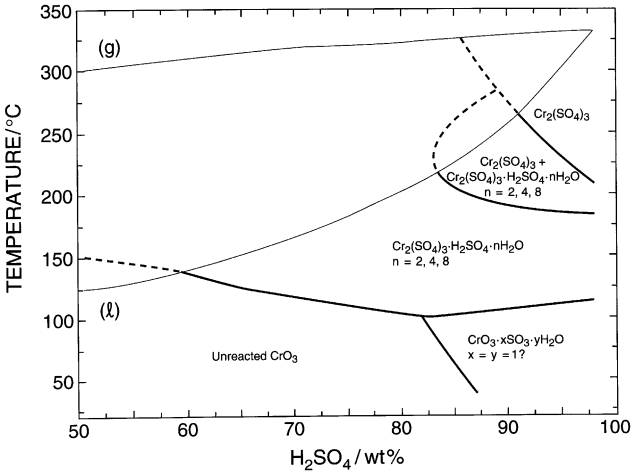

Fig. 1. Schematic summary (based on the outcome of some 100 individual syntheses with long reaction periods) of products resulting from reaction between CrO_3 and H_2SO_4 as function of H_2SO_4 concentration and reaction temperature. Tentative phase fields for the products are marked with thicker lines, whereas thinner lines reproduce the 50–98 wt% section of the boiling-point diagram for (pure) H_2O–H_2SO_4 according to Ref. [28]. Concerning $Cr_2(SO_4)_3 \cdot H_2SO_4 = 2CrH(SO_4)_2$ see text.

half-a-year darkens the color further, makes the greenish stain more evident, and gives the solution a more distinct oily consistency. At the brown-colored stage a brown solid phase can be filtered off, but this product is so hygroscopic that in less than a minute it reverts to CrO_3. (CrO_3 is also obtained after washing of the brown product with glacial acetic acid.) In line with earlier findings [1–8], the present results confirm that the brown product contains chromium(VI) and sulfate, and we feel tempted to conclude that it really lives up to the name chromic–sulfuric acid, viz. H_2CrSO_7. However, we leave this aspect here, but hope to be able to return to it with better means for isolation and characterization of such hygroscopic species.

The green solutions, the green products obtained from these, and green deposits on the brown product (see above) proved to contain Cr^{III}. The particle size of such derived solid products was assessed to around 20 μm and PXD suggested an amorphous character. The stipulation of the valence state of chromium was therefore based on magnetic susceptibility measurements and TG analyses. The TG data comply with the gross formula $Cr_2(SO_4) \cdot H_2SO_4$ plus some adhered acidic motherliquid on the particles. (The adhered acid evaporates in a poorly defined TG stage between 50°C and ca. 275°C, whereas "amorphous" $Cr_2(SO_4) \cdot H_2SO_4$ decomposes to $Cr_2(SO_4)_3$ between ca. 300°C and 400°C and further to Cr_2O_3 between 575°C and 675°C.) The thermomagnetic data show that the compound in question becomes antiferromagnetic below 9 K and follows Curie–Weiss law above this temperature with

$\mu_P = 3.85(1)\mu_B$ per assumed $CrH(SO_4)_2$ formula unit and $\Theta = -3.0(6)$ K.

Above some 100°C and 60 wt% H_2SO_4 Cr^{VI} is reduced to Cr^{III}, but apart from at high H_2SO_4 concentrations and high temperatures where $Cr_2(SO_4)_3$ rules as the sole product, two-phase mixtures were obtained of $Cr_2(SO_4)_3$ and $Cr_2(SO_4)_3 \cdot H_2SO_4 \cdot nH_2O$ ($n = 2$, 4 or 8, gross formulae; $n = 0$ is difficult to assess due to its micro-crystalline state; see above and below) or of the latter with different n values (see Fig. 1). (In some cases the products even proved to contain three of the said compounds.) The difficulties encountered with regard to phase-pure products are attributed to kinetic factors like concentration fluctuations in the reaction vessel, and to the fact that once a wrong, but nearly equilibrium situation has been established its rectification requires redissolving of the product. However, on application of the H_2SO_4 concentrations and temperatures specified in the footnote to Table 1 it was possible to prepare samples of $Cr_2(SO_4)_3 \cdot H_2SO_4 \cdot nH_2O$, $n = 2$, 4 and 8 which were pure enough to justify attempts to characterize them by PXD and TG.

The entire series $Cr_2(SO_4)_3 \cdot H_2SO_4 \cdot nH_2O$, $n = 0$, 2, 4, and 8 are to smaller or larger extent hygroscopic (in combination with, or owing to, adhered acidic mother-liquid) which leads to blurred TG diagrams. The TG data are therefore only referred to in the text (quoting start and end temperatures for a given decomposition stage at a heating rate of 10°C min^{-1} and N_2 atmosphere) and not reproduced as illustrations (which, however, may be obtained from the authors upon request). The PXD samples could, on the other hand, be prepared and examined under a protective atmosphere.

$Cr_2(SO_4)_3 \cdot H_2SO_4 \cdot 2H_2O$ loses H_2SO_4 and H_2O in one composite state, most distinct from ca. 350°C to 450°C, the TG curve then goes through $Cr_2(SO_4)_3$ as a somewhat indistinct holding composition which in turn is followed by the decomposition to Cr_2O_3 (completed at ca. 700°C). The TG curve for $Cr_2(SO_4)_3 \cdot H_2SO_4 \cdot 4H_2O$ closely resembles that for $Cr_2(SO_4)_3 \cdot H_2SO_4 \cdot 2H_2O$ except that here the latter composition appears as an indistinct holding stage between ca. 100°C and 200°C. The most distinct TG signature of $Cr_2(SO_4)_3 \cdot H_2SO_4 \cdot 2H_2O$ is found as a virtually composition invariant stage between ca. 150°C and 225°C (ca. 100–190°C for heating at 0.5°C min^{-1}) in the TG curve for $Cr_2(SO_4)_3 \cdot H_2SO_4 \cdot 8H_2O$. The TG data shows that $Cr_2(SO_4)_3 \cdot H_2SO_4 \cdot 8H_2O$ itself is thermally stable up to ca. 100°C (ca. 75°C at 0.5°C min^{-1}), where the composition invariant stage is interrupted by the onset of decomposition to $Cr_2(SO_4)_3 \cdot H_2SO_4 \cdot 2H_2O$. The further decomposition of $Cr_2(SO_4)_3 \cdot H_2SO_4 \cdot 2H_2O$ to $Cr_2(SO_4)_3$ takes place in one continuous step, although the TG curve gives indication that (say) $Cr_2(SO_4)_3 \cdot H_2SO_4$ may occur as an intermediate at around 300°C. Examination of $Cr_2(SO_4)_3 \cdot H_2SO_4 \cdot 8H_2O$ by high-temperature PXD (and r.t. PXD studies of heat-treated samples) confirmed only $Cr_2(SO_4)_3 \cdot H_2SO_4 \cdot 2H_2O$ (ca. 100–200°C) and $Cr_2(SO_4)_3$ (ca. 300–500°C, the latter temperature complying with the TG data for $Cr_2(SO_4)_3$ prepared by chemical transport reaction) as crystalline intermediates. However, the high-temperature PXD diagrams taken at around 250°C (and r.t. PXD examination of samples heat treated in the same temperature range) revealed only amorphous material(s), findings which concur with the PXD-amorphous products of $Cr_2(SO_4)_3 \cdot H_2SO_4$ discussed above.

The TG curve of $Cr_2(SO_4)_3 \cdot 14H_2O$ show a convincing sign (viz. a distinct holding plateau at exactly the right composition) of the occurrence of $Cr_2(SO_4)_3 \cdot 12H_2O$ as an intermediate decomposition product between ca. 60°C and 100°C, but again high-temperature PXD examination detected only PXD-amorphous material(s). The further decomposition progresses,

Table 1
Unit-cell dimensions (e.s.d.s in parentheses) at r.t. for sulfates and mixed sulfates–hydrogen sulfates of chromium(III) obtained by treatment of CrO_3 in concentrated H_2SO_4

Compound[a]	Symmetry	a (Å)	b (Å)	c (Å)	Remark
$Cr_2(SO_4)_3$ [17]	Trigonal, $R\bar{3}$	8.143	8.143	21.983	PXD data; $d^b_{obs} = 2.99(7)$ g cm^{-3}
		8.1116(2)	8.1116(2)	21.9356(6)	PND data, 10 K[c]
$Cr_2(SO_4)_3 \cdot H_2SO_4 \cdot 2H_2O$	Trigonal, $R\bar{3}$	4.749	4.749	23.535	$K[Sb(PO_4)_2]$-type [29] structure[d]
$Cr_2(SO_4)_3 \cdot H_2SO_4 \cdot 4H_2O$					One axis 10.329 Å ?
$Cr_2(SO_4)_3 \cdot H_2SO_4 \cdot 8H_2O$	Orthor., *Pnma*	9.6071(6)	18.312(2)	5.3994(3)	$(H_5O_2)[Fe(H_2O)_2(SO_4)_2]$-type [32] structure[e]
$Cr_2(SO_4)_3 \cdot 14H_2O$					Not indexed[f]

[a] Synthesis concentration (wt% H_2SO_4) and temperature (°C) for the compounds in the said order: 95, 250; 80, 180; 65, 140; 65, 150 [obtained only once, see text]; 55, r.t. (see Experimental).

[b] Measured pycnometrically at 20.5°C with a saturated solution of $Cr_2(SO_4)_3$ in 95 wt% H_2SO_4 as displacement liquid.

[c] Rhombohedral description $a = 8.6843(5)$ Å, $\alpha = 55.71(5)°$.

[d] Isostructural with $(H_3O)[M(SO_4)_2]$, M = Al, Ga, In, Tl [30,31]; in rhombohedral description $a = 2.742$ Å, $\alpha = 60.0°$.

[e] Isostructural with $(H_5O_2)[M(H_2O)_2(SO_4)_2]$, M = Al, Ga, In, Tl, V, Mn, Fe [30,32–35].

[f] PXD pattern corresponds to PDF No. 49-1000 [36].

according to TG, as one continuous process all the way to Cr_2O_3. However, in the vicinity of the composition $Cr_2(SO_4)_3$ the TG curve has a wide portion from ca. 150°C to 550°C with a relatively low weight-loss rate, and high-temperature PXD data from this temperature range confirm that $Cr_2(SO_4)_3$ rules as the only crystalline phase.

$Cr_2(SO_4)_3$, $Cr_2(SO_4)_3 \cdot H_2SO_4 \cdot 2H_2O$, and $Cr_2(SO_4)_3 \cdot H_2SO_4 \cdot 8H_2O$ are conveniently characterized by their crystal structures (see Table 1 and below). The PXD diagrams of $Cr_2(SO_4)_3 \cdot H_2SO_4 \cdot 4H_2O$ contained only a few low-angle ($2\theta < 60°$) reflections of which the first six could be indexed in terms of only one axis, e.g., $c = 10.329$ Å [corresponding to $0\,0\,l$ with $l = 1(100)$, 2(4), 3(4), 4(6), 6(2), and 7(1), the numbers in the parentheses giving relative intensities (in %)]. These findings could indicate extreme preferred orientation of crystallites, but PXD diagrams collected in reflection and transmission geometry gave virtually identical patterns. Despite the lacking structural insight we take the liberty to suggest that $Cr_2(SO_4)_3 \cdot H_2SO_4 \cdot 4H_2O$ in reality is an oxonium or aquaoxonium derivative of chromium sulfate in line with the findings for $Cr_2(SO_4)_3 \cdot H_2SO_4 \cdot 2H_2O$ and $Cr_2(SO_4)_3 \cdot H_2SO_4 \cdot 8H_2O$. The structural characterization of $Cr_2(SO_4) \cdot 14H_2O$ has been limited to ascertaining that the present PXD data concur with the PDF database [36].

3.2. Crystal and magnetic structures of $Cr_2(SO_4)_3$

The crystal structure of $Cr_2(SO_4)_3$ has been determined [17] as recently as 1993 on the basis of high-quality single-crystal data and the only argument for a redetermination is that we found that it undergoes a paramagnetic-to-antiferromagnetic transition at $T_N = 14.5(3)$ K [Curie–Weiss law satisfied: $\Theta = -7.8(5)$ K; $\mu_P = 3.708(3)$ μ_B corresponding (according the "spin-only" approximation) to $S_P = 1.420(2)$]. PND data collected at 10 K show that the metrics of the magnetic unit cell is in conformity with that of the nuclear. However, each of the two six-fold chromium positions (Cr(1) and Cr(2)) of the nuclear unit cell is split in two three-fold positions (Cr(1A) and Cr(1B); Cr(2A) and Cr(2B): corresponding to a change from space group $R\bar{3}$ to $R3$) in order to account for the antiferromagnetic ordering of the moments. The PND data (Fig. 2) were subjected to a combined Rietveld refinement of the variable nuclear and magnetic structural parameters and the results are listed in Table 2 (unit-cell dimensions in Table 1).

The present values for the nuclear fractional co-ordinates are generally in very good agreement with those of Dahmen and Gruehn [17] (for about half of the parameters within one standard deviation and at most within six standard deviations). Although it should be borne in mind that the present data refer to 10 K and those of Dahmen and Gruehn to r.t. (with significant differences in unit-cell dimensions) it is appropriate to refer to the latter authors [17] for interatomic distances and angles, structure illustrations, and descriptions. (The present data for the nuclear structure give rise to bond valences [37] of 3.18 and 3.35 for Cr(1) and Cr(2), respectively, and 5.99 for S.)

The antiferromagnetic structure of $Cr_2(SO_4)_3$ is illustrated in Fig. 3, where only the chromium atoms

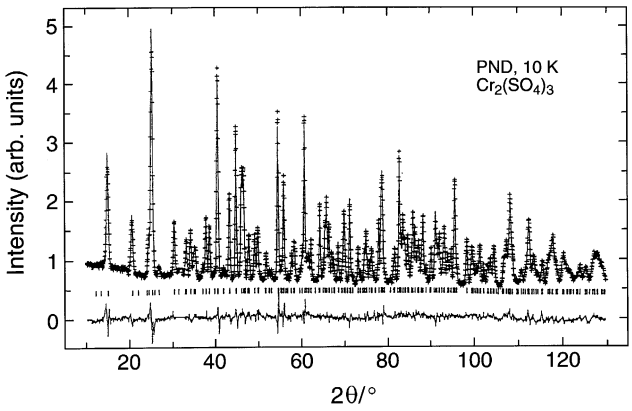

Fig. 2. Rietveld refinements (upper line; the 2θ range 31–33° excluded from the refinements) of PND data (crosses; $\lambda = 1.555$ Å; 2400 data points, 562 Bragg reflections; collected at 10 K) for $Cr_2(SO_4)_3$. Positions of Bragg reflections are marked with bars. The difference between observed and calculated intensities is shown by the bottom line.

Table 2
Refined nuclear and magnetic structure parameters for $Cr_2(SO_4)_3$ at 10 K (hexagonal setting, unit-cell dimensions in Table 1; $\chi^2 = 1.92$, $R_{wp} = 0.052$, $R_{nucl} = 0.040$, and $R_{magn} = 0.075$); antiferromagnetic splitting of the Cr site (co-ordinate notation z_{Spl}): subsite A corresponds to nuclear z, subsite B to $1 - z$

Nuclear cell ($R\bar{3}$)					
Atom	Site	x	y	z	HB_{Iso}/Å^2
Cr(1)	6*c*	0	0	0.1451(5)	0.24(7)
Cr(2)	6*c*	0	0	0.3486(5)	0.24(7)
S	18*f*	0.2874(7)	0.2840(7)	0.2502(3)	0.358(1)
O(1)	18*f*	0.8710(4)	0.3425(3)	0.1408(1)	0.45(2)
O(2)	18*f*	0.8083(4)	0.2488(4)	0.0343(1)	0.45(2)
O(3)	18*f*	0.0382(3)	0.2080(4)	0.0887(1)	0.45(2)
O(4)	18*f*	0.1047(4)	0.5247(4)	0.0670(1)	0.45(2)

Magnetic cell ($R3$; site 3*a*)				
Atom	z_{Spl}	μ^a_{xy}/μ_B	μ_z/μ_B	μ_{AF}/μ_B
Cr(1A)	0.1451(5)	−2.2(2)	1.5(3)	2.7(5)
Cr(1B)	0.8549(5)	2.2(2)	−1.5(3)	2.7(5)
Cr(2A)	0.3486(5)	2.2(2)	−1.5(3)	2.7(5)
Cr(2B)	0.6514(5)	−2.2(2)	1.5(3)	2.7(5)

[a] The direction of the moments within the *ab* plane is undetermined.

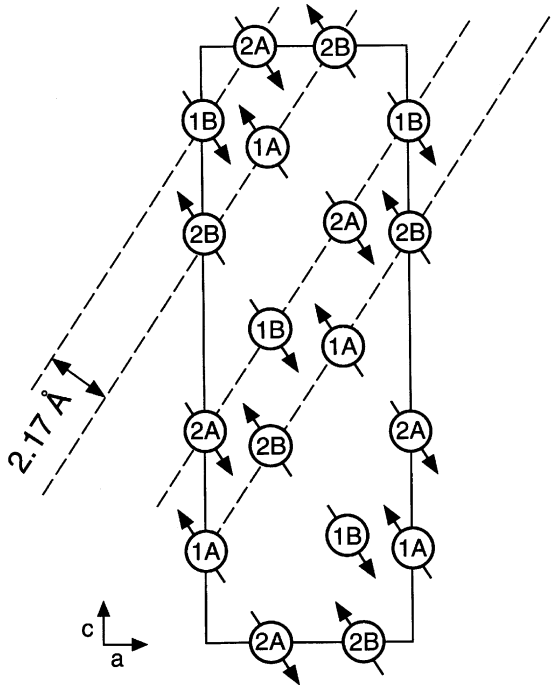

Fig. 3. The antiferromagnetic structure of $Cr_2(SO_4)_3$ projected on (010) showing only the locations of Cr (labeled in accordance with Table 2). Arrows indicate direction of magnetic moments (note: undetermined within the *ab* plane), continuous lines show unit-cell outline, and broken lines assign planes with parallel oriented moments.

and their moment orientations are shown for simplicity. The chromium atoms are confined in CrO_6 octahedra, which, in turn, are mutually connected via corner-sharing SO_4 tetrahedra. Focussing only on the CrO_6 octahedra, these can be said to be arranged in planes parallel to $(3, 0, -6)$. The moments of Cr(1) and Cr(2) within a given such plane are aligned parallel whereas those in the closest neighboring planes (ca. 2.17 Å apart) are arranged antiparallel. The shortest interatomic Cr–Cr distances between antiferromagnetic-arranged moments are in the range $\sim$4.52–4.80 Å, whereas the ferromagnetic-aligned moments are further apart ($\sim$5.86–8.12 Å). Direct Cr–Cr magnetic exchange interactions are thus excluded and the magnetic information must accordingly be conveyed indirectly via ...Cr–O–S–O–Cr... pathways.

The antiferromagnetic moment, $\mu_{AF} = 2.7(5)\mu_B$, corresponds to a spin-quantum number ($S_{AF} = \mu_{AF}/2$) which is some 5% smaller than that obtained by the magnetic susceptibility measurements. This distinction is easily explained as a consequence of the fact that the PND data collection was performed (at 10 K) very close to $T_N = 14.5(3)$ K. The fact that the paramagnetic-based spin-quantum number ($S_P = 1.420(2)$) also deviates from $S = \frac{3}{2}$ expected for a d^3 state appears to reflect the inherent imperfection of the "spin-only" approximation.

3.3. Crystal structure of $Cr_2(SO_4)_3 \cdot H_2SO_4 \cdot 2H_2O$

As already discussed it proved impossible to prepare completely phase-pure $Cr_2(SO_4)_3 \cdot H_2SO_4 \cdot 2H_2O$ with the methods used in this study. However, our somewhat imperfect samples gave PXD data which were fully satisfactory to confirm that this compound belongs to the isostructural series $(H_3O)[M(SO_4)_2]$, M = Al, Ga, In, Tl [30,31]. The PXD data were not good enough to justify refinements, but simulated PXD diagrams with positional parameters from Ref. [31] suggest that the latter co-ordinates also represent passable values for $Cr_2(SO_4)_3 \cdot H_2SO_4 \cdot 2H_2O$, which accordingly correctly should be ascribed the formula $(H_3O)[Cr(SO_4)_2]$.

Magnetic susceptibility measurements on the present samples of $(H_3O)[Cr(SO_4)_2]$ confirm the trivalent state of chromium ($\mu_P = 3.82(3)\mu_B$, $\Theta = -9.2(9)$ K) and indicate that this compound, like the other chromium sulfates studied, undergoes a paramagnetic-to-antiferromagnetic transition at around 10 K.

3.4. Crystal structure of $Cr_2(SO_4)_3 \cdot H_2SO_4 \cdot 8H_2O$

The in-house-collected PXD data immediately made it clear that $Cr_2(SO_4)_3 \cdot H_2SO_4 \cdot 8H_2O$ belongs to the isostructural series $(H_5O_2)[M(H_2O)_2(SO_4)_2]$, M = Al, Ga, In, Tl, V, Mn, Fe [30,32–35]. Moreover, magnetic susceptibility measurements showed that this compound is subjected to a paramagnetic-to-antiferromagnetic transition at $T_N = 9.0$ K (above which temperature Curie–Weiss law is satisfied with $\Theta = -12.9(7)$ K and $\mu_P = 3.782(6)\mu_B$ [corresponding to $S_P = 1.456(3)$ according to the "spin-only" approximation]. A room- and low-temperature PND investigation would therefore have been highly appropriate, but unfortunately there was no D_2SO_4 available for synthesis of deuterated samples. In this situation, it was decided to perform structural refinements on the basis of synchrotron PXD data (Fig. 4). The atomic co-ordinates for the iron analogue [32] were used as input parameters for the Rietveld refinements which progressed smoothly for Cr, S, and the oxygen atoms co-ordinated to chromium and sulfur [viz. O(1)–O(5)] whereas the oxygen atoms of the aquaoxonium ($H_5O_2^+$) units were first located from difference-Fourier maps. (The layer character of the structure along [010] leads to a degree of preferred orientation of the crystallites of the PXD specimens which is taken into account in the refinements.) The refinements of the thus established co-ordinates for O(6)–O(8) immediately brought out that the oxygen atoms of the $H_5O_2^+$ units of the present powder samples of $Cr_2(SO_4)_3 \cdot H_2SO_4 \cdot 8H_2O$ are subject to positional disorder, and fractional occupation numbers (Table 3) were introduced to account for this imperfection. (The disorder, which occurs for M = Cr and Fe [32] of this isostructural series, and appears to be lacking for

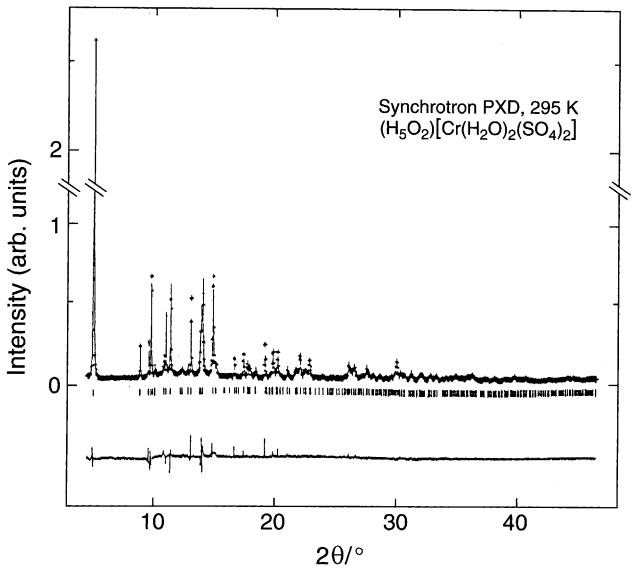

Fig. 4. Rietveld refinements (upper line) of synchrotron PXD data (crosses; $\lambda = 0.80202$ Å; 3500 data points, 587 Bragg reflections; collected at 295 K) for $Cr_2(SO_4)_3 \cdot H_2SO_4 \cdot 8H_2O$. Positions of Bragg reflections are marked with bars. The difference between observed and calculated intensities is shown by the bottom line.

M = Al [35] and Mn [34], is likely to result from the preparational procedures rather than reflecting something specific for the former elements and/or structures. Besides, according to the occupation numbers the disorder in the chromium compound appears to differ from that in the iron analogue.)

Instructive illustrations of the $(H_5O_2)[M(H_2O)_2(SO_4)_2]$ structures are found in Refs. [32–35] and are therefore not repeated here. The two-dimensional layer structure of $(H_5O_2)[Cr(H_2O)_2(SO_4)_2]$ consists of corner-shared CrO_6 octahedra and SO_4 tetrahedra. The two Cr–O(5) distances [2.042(6) Å], which reflect bonding to the oxygens of water molecules, are significantly larger than the oxygen linkages [2 × Cr–O(1) 1.945(7); 2 × Cr–O(2) 1.926(8) Å] to the SO_4 groups. [The overall Cr bond valence is 3.08 and the O–Cr–O bond angles fall in the range 86.2(6)–93.8(6)°.] The bonding S–O distances are almost identical [1.481(1)–1.484(1) Å; overall S bond valence 5.87] whereas the O–S–O bond angles vary somewhat [104.3(9)–116(1)°]. The aquaoxonium units in the structure of $Cr_2(SO_4)_3 \cdot H_2SO_4 \cdot 8H_2O$ are intercalated between the $[Cr(H_2O)_2(SO_4)_2]$ layers as opposed to the situation in the structures of $CrH(SO_4)_2 \cdot 7H_2O$ and $Cr_4H_2(SO_4)_7 \cdot 24H_2O$ [38,39] where oxonium units appears to be associated with sulfate groups.

4. Concluding remarks

The use of CrO_3 as the chromium reactant may at first glance look odd since the bulk of the work has concerned Cr^{III} sulfates. However, our delibrations were as follows: Cr_2O_3 is well known as insoluble in cold or hot water, acids, and alkali (e.g., see under-graduate student textbooks). Insoluble is clearly a too categorical word, but even with a small solubility of Cr_2O_3 in concentrated H_2SO_4 the reaction rate would be low and reaction products would be contaminated with unreacted starting material. The use of other Cr^{III} compounds as reactant was considered undesirable on account of the contamination risks. The use of CrO_3 as reactant has, besides the efficient on-site generation of Cr^{III} species and the associated facilitation for the reaction rate, the additional advantage of providing a coarse picture of the stability of Cr^{VI} in H_2SO_4 at different temperatures and concentrations (Fig. 1).

A fair amount of the information on the present chromium(III) sulfate samples has been surveyed by magnetic susceptibility measurement. The general trend is that the trivalent state of chromium has been confirmed and perhaps more unexpected all tested specimens gave clear indications of a paramagnetic-to-antiferromagnetic transition in the vicinity of 10 K. The latter feature was also observed for specimens which we initially had characterized as PXD amorphous. Hence, the structural state of these products should rather be referred to as micro-crystalline.

Two of the three new acidic chromium(III) sulfates which have been identified in this study $(H_3O)[Cr(SO_4)_2]$ and $(H_5O_2)[Cr(H_2O)_2((SO_4)_2]$ have protons attached to water molecules [and this applies almost certainly also to $Cr_2(SO_4)_2 \cdot H_2SO_4 \cdot 4H_2O$ (gross formula)]. An interesting, but not yet properly answered question, is why the protons prefer association with H_2O or $2H_2O$ rather than with the CrO_6 or SO_4 units of the crystal structures. The explanation has clearly something to do with the relative acid–base strengths of the just mentioned structural fragments, and in this connection it should be recalled that Cr_2O_3,

Table 3
Refined crystal structure of $Cr_2(SO_4)_3 \cdot H_2SO_4 \cdot 8H_2O\{= 2(H_5O_2)[Cr(H_2O)_2(SO_4)_2]\}$ at 295 K (space group *Pnma*, unit-cell dimensions in Table 1, $\chi^2 = 2.85$, $R_{wp} = 0.057$, $R_p = 0.043$); hydrogen positions not included

Atom	Site	x	y	z	HB_{Iso}/Å^2
Cr	4*a*	0	0	0	0.34(2)
S	8*d*	0.233(2)	0.0886(3)	0.2879(4)	1.66(2)
O(1)	8*d*	0.3239(6)	0.0236(7)	0.3415(8)	0.9(2)
O(2)	8*d*	0.094(1)	0.058(1)	0.246(1)	0.9(2)
O(3)	8*d*	0.284(1)	0.125(1)	0.057(2)	0.9(2)
O(4)	8*d*	0.226(2)	0.136(2)	0.511(2)	0.9(2)
O(5)	8*d*	0.494(2)	0.0878(7)	0.733(2)	0.9(2)
O(6)	4*c*	0.647(3)	0.25	0.556(4)	2.7(3)[a]
O(7)	4*c*	0.388(2)	0.25	0.566(4)	2.7(3)[b]
O(8)	4*c*	0.44(1)	0.25	0.09(1)	2.7(3)[c]

[a] Occupation number 0.82(2).
[b] Occupation number 0.98(3).
[c] Occupation number 0.16(2).

like Al_2O_3 and other oxides which form acidic trivalent metal sulfates, is classified as an amphoteric substance. However, the full revelation of the explanation is long in coming.

References

[1] P.A. von Bolley, Liebigs Ann. Chem. 56 (1845) 113.
[2] A.W. Rakowsky, D.N. Tarassenskow, Z. Anorg. Chem. 174 (1928) 91.
[3] A.M. Gay-Lussac, Ann. Chim. Phys. 16 (1821) 102.
[4] J. Fritsche, J. Prakt. Chem. 19 (1840) 176.
[5] A. Schrötter, Ann. Phys. 59 (1843) 616.
[6] K. Pietet, Bull. Soc. Chim. Fr. 3 (1908) 1114.
[7] J. Meyer, V. Stateczny, Z. Anorg. Chem. 122 (1922) 1.
[8] L.F. Gilbert, H. Buckley, I. Masson, J. Chem. Soc. 121 (1922) 1934.
[9] L.-J. Simon, C. R. Acad. Sci. Paris 175 (1922) 768.
[10] V.V. Ipatiev, V.G. Tronev, Zh. Prikl. Khim. (St. Petersburg) 6 (1933) 832.
[11] H.C. Snethlage, Rec. Trav. Chim. Pays-Bas. 55 (1936) 874.
[12] A. Schrötter, Ann. Phys. 53 (1841) 513.
[13] E.R. Caley, J. Am. Chem. Soc. 54 (1933) 3947.
[14] D. Taylor, J. Chem. Soc. (1953) 2502.
[15] P.A. Kokkoros, Tschermaks Mineral. Petrogr. Mitt. 10 (1965) 45.
[16] A. Thrierr-Sorel, A. Roux, C. R. Acad. Sci. Ser. C 266 (1968) 457.
[17] T. Dahmen, R. Gruehn, Z. Kristallogr. 204 (1993) 57.
[18] O. Söhnel, P. Nowotný, Densities of Aqueous Solutions of Inorganic Substances, Elsevier, New York, 1985.
[19] M. Traube, Liebigs Ann. Chem. 66 (1848) 65.
[20] P.-E. Werner, Program SCANPI-6, Institute of Inorganic Chemistry, Stockholm University, 1988.
[21] P.-E. Werner, L. Erikson, M. Westdahl, Program TREOE, Version 5, Institute for Inorganic Chemistry, Stockholm University, 1988 (see also J. Appl. Crystallogr. 18 (1985) 367).
[22] N.O. Ersson, Program CELLKANT, Chemical Institute, Uppsala University, 1981.
[23] WIN-INDEX Professional Powder Indexing, Version 3.0, Siemens AG Analytical X-ray System AUT, Karlsruhe, 1996.
[24] B.C. Hauback, H. Fjellvåg, O. Steinsvoll, K. Johansson, O.T. Buset, J. Jørgensen, J. Neutron Res. 8 (2000) 215.
[25] D.B. Wiles, A. Sakthivel, R.A. Young, Program DBW3.2S, School of Physics, Georgia Institute of Technology, Atlanta, GA, 1988.
[26] A.C. Larson, R.B. von Dreele, Program GSAS, General Structure Analysis System, LANSCE, MS-H 805, Los Alamos National Laboratory, Los Alamos, NM, 1998.
[27] A.F. Christiansen, H. Fjellvåg, A. Kjekshus, B. Klewe, J. Chem. Soc. Dalton Trans. (2001) 806.
[28] Gmelins Handbuch der Anorganischen Chemie, System-Nummer 9: Schwefel, Verlag Chemie, Weinheim, 1960, p. 677.
[29] Y. Piffard, S. Oyetola, S. Courant, A. Lachgar, J. Solid State Chem. 60 (1985) 209.
[30] J. Tudo, M. Tudo, B. Jolibois, R. Perret, Rev. Chim. Mineral. 11 (1974) 489.
[31] T. Fischer, B. Eisenmann, R. Kneip, Z. Kristallogr. 211 (1996) 465.
[32] K. Merciter, Tschermaks Mineral. Petrogr. Mitt. 21 (1974) 216.
[33] J. Tudo, B. Jolibois, G. Laplace, G. Nowagrocki, F. Abraham, J. Appl. Crystallogr. 11 (1978) 707; Acta Crystallogr., Section B 35 (1979) 1580.
[34] F.M. Chang, M. Jansen, D. Schmitz, Acta Crystallogr. Section C 39 (1983) 1497.
[35] T. Fischer, B. Eisenmann, R. Kneip, Z. Kristallogr. 211 (1996) 466.
[36] M. Tourchi, Rep.-Geol. Mineral Geol. Surv. Iran No. 2 (1993).
[37] N.E. Brese, M. O'Keeffe, Acta Crystallogr. Section B 47 (1991) 192.
[38] T. Gustafsson, J.-O. Lundgren, I. Olovsson, Acta Crystallogr. Section B 33 (1977) 2373.
[39] T. Gustafsson, J.-O. Lundgren, I. Olovsson, Acta Crystallogr. Section B 36 (1980) 1323.